Journal of Hazardous Materials 186 (2011) 1042–1049

Contents lists available at ScienceDirect

Journal of Hazardous Materials

journal homepage: www.elsevier.com/locate/jhazmat

Defluoridation from aqueous solutions by nano-alumina: Characterization and sorption studies

Eva Kumar[b], Amit Bhatnagar[a,b,*], Umesh Kumar[c], Mika Sillanpää[d]

[a] Institute of Environmental Technology and Energy Economics, Technische Universität Hamburg-Harburg (TUHH), 21073 Hamburg-Harburg, Germany
[b] LSRE – Laboratory of Separation and Reaction Engineering, Departamento de Engenharia Química, Faculdade de Engenharia da Universidade do Porto (FEUP), Rua Dr. Roberto Frias, 4200-465 Porto, Portugal
[c] Department of Chemistry, National Cheng Kung University, Tainan 701, Taiwan, ROC
[d] Faculty of Technology, Lappeenranta University of Technology, Patteristonkatu 1, FI-50100 Mikkeli, Finland

ARTICLE INFO

Article history:
Received 25 June 2010
Received in revised form
12 November 2010
Accepted 24 November 2010
Available online 3 December 2010

Keywords:
Fluoride removal
Nano-alumina
Adsorption isotherms
Sorption mechanism
pH

ABSTRACT

The present study was conducted to evaluate the feasibility of nano-alumina (Al_2O_3) for fluoride adsorption from aqueous solutions. The nature and morphology of pure and fluoride-sorbed nano-alumina were characterized by SEM with EDX, XRD, and FTIR analysis. Batch adsorption studies were performed as a function of contact time, initial fluoride concentration, temperature, pH and influence of competing anions. Fluoride sorption kinetics was well fitted by pseudo-second-order model. The maximum sorption capacity of nano-alumina for fluoride removal was found to be 14.0 mg g^{-1} at 25 °C. Maximum fluoride removal occurred at pH 6.15. The fluoride sorption has been well explained using Langmuir isotherm model. Fluoride sorption was mainly influenced by the presence of PO_4^{3-}, SO_4^{2-} and CO_3^{2-} ions.

1. Introduction

Fluoride contamination in drinking water due to natural and anthropogenic activities has been recognized as one of the major problems worldwide [1]. Besides the natural geological sources for fluoride enrichment in groundwater, the discharge of the wastewaters from various industries, e.g., drugs, cosmetics, semiconductor manufacturing, coal power plants, glass and ceramic production, electroplating, rubber, fertilizer manufacturing, also contaminate the surface and groundwater with fluoride [2,3]. Fluoride is classified as one of the human consumption water contaminant by the World Health Organization (WHO), which cause large-scale health problems through drinking water exposure, in addition to arsenic and nitrate [4]. Consuming excess fluoride through drinking water often leads to skeletal fluorosis, causing debilitating bone structure disease, as well as discoloration and mottling of teeth, cancer or adverse effects on the brain and kidney [5]. It was estimated that globally more than 70 million people are suffering from fluorosis. WHO has set the safe limit of fluoride concentration in drinking water as 1.5 mg L^{-1}.

Several methods have been applied to remove excessive fluoride from aqueous solution, such as adsorption [6,7], precipitation [8], ion-exchange [9], electrodialysis [10] and reverse osmosis [11]. Among these methods, adsorption is still one of the most extensively used methods, because of its simplicity and the availability of a wide range of adsorbents. Various materials such as activated alumina [6], clay [12], soil [13], bone char [14], zeolites [15], granular ferric hydroxide [16] and biosorbent [17] have been successfully tested for defluoridation of drinking water.

It has been well reported in literature that metal oxides (especially iron and aluminium) have been found to be excellent sorbents for anions removal from aqueous solutions as generally they carry positive surface charge and negatively charged anions are sorbed on the positively charged surface of metal oxides by electrostatic attraction. In the natural environment, fluoride has been proven to be strongly adsorbed onto various aluminium-containing mineral surfaces [18]. United States Environmental Protection Agency (US EPA) has also recommended the use of activated alumina as an adsorbent for defluoridation [19]. Conventionally, aluminium based micron-sized adsorbents have been employed for the removal of fluoride, however, in recent years use of nano-sized materials has emerged as one of the appealing technology for water treatment. Nanomaterials have a number of key physico-

* Corresponding author at: LSRE – Laboratory of Separation and Reaction Engineering, Departamento de Engenharia Química, Faculdade de Engenharia da Universidade do Porto (FEUP), Rua Dr. Roberto Frias, 4200-465 Porto, Portugal.
E-mail addresses: dr.amit10@gmail.com, amit_b10@yahoo.co.in (A. Bhatnagar).

0304-3894/$ – see front matter © 2010 Elsevier B.V. All rights reserved.
doi:10.1016/j.jhazmat.2010.11.102

chemical properties (e.g. larger surface area than bulk particles, enhanced reactivity and self-assembly) that make them particularly attractive as separation media for water purification [20,21]. As the sorption or binding sites reside only on the surface, nanoscale metal oxide particles with a very high surface-to-volume ratio offer significantly enhanced sorption capacity and shorter diffusion route [22–24]. However, only a few reports are available in literature dealing with the applications of nano-scale metal oxides for the removal of fluoride and other anions from water [21,24–27]. In this perspective, it was thought desirable to test the potential of nano-alumina for fluoride removal as alumina and aluminum containing compounds have high affinity toward fluoride but no detailed studies are reported on the defluoridation of water using nano-alumina. In this study we combined the properties of metal oxides at nano-scale to achieve the enhanced removal of fluoride from water.

In the present study, the sorption feasibility of nano-alumina has been assessed for fluoride removal from aqueous solution. The physical and chemical characterization of nano-alumina by scanning electron micrographs (SEM), X-ray diffraction (XRD), Fourier transform infra-red spectroscopy (FTIR), energy dispersive X-ray analysis (EDX), and Brunauer–Emmett–Teller (BET), were conducted and further the potential of the nano-alumina was evaluated for fluoride removal. Defluoridation studies were conducted under various experimental conditions, such as pH, contact time, initial fluoride concentrations, temperature, and the presence of competing anions. The data from the experiments were fitted with different models to identify the adsorption mechanism. The results have been thoroughly discussed which would help in the better understanding of defluoridation mechanism by nano-alumina.

2. Materials and methods

2.1. Materials

Nano-alumina was purchased from Sigma–Aldrich. Fluoride stock solution was prepared by dissolving NaF (Sigma–Aldrich) in deionized (DI) water. Standards and fluoride spiked samples at a required concentration range were prepared by appropriate dilution of the stock solution with DI water. All reagents used were of analytical reagent grade.

2.2. Characterization of the sorbent

Nitrogen adsorption/desorption isotherms were obtained using a BEL Japan Inc. Belsorp-Max surface area analyzer at 77 K. The morphology of the sorbent was determined by scanning electron microscopy (SEM) using Quanta 200 (FEI, Netherlands) field-emission gun (FEG) scanning electron microscope. The X-ray diffraction (XRD) pattern of the nano-alumina was obtained using a Bruker AXS D8 Advance X-ray diffractometer. FTIR spectra of the sorbent was collected using Nicolet 8700 FTIR spectrometer (Thermo Instruments, USA).

2.3. Determination of point of zero charge

Solid addition method [28] was used to determine the zero surface charge characteristics (pH_{pzc}) of nano-alumina using 0.1 M KCl solution along with 20 mg L^{-1} fluoride and a blank. Forty milliliters of KCl and fluoride solutions of desired strengths were transferred to a series of 50 mL capped glass tubes. The initial pH ($pH_{initial}$) of the solutions was adjusted in the range of 2.0–12.0 by adding 0.1 M HCl and 0.1 M NaOH solutions. The total volume of the solution in each tube was adjusted exactly to 50 mL by adding KCl and fluoride solution of the same strength. Further, 0.5 g of sorbent was added to all tubes and the suspensions were then equilibrated for 48 h. After completion of the equilibration time, the solutions were filtered and final pH values (pH_{final}) of the filtrates were measured again. The difference between the initial and final pH (pH_f) values ($\Delta pH = pH_i - pH_f$) was plotted against the pH_i. The point of intersection of the resulting curve with abscissa, at which $\Delta pH = 0$, gave the point of zero charge.

2.4. Fluoride analysis

The concentration of fluoride in the solutions was determined by ion chromatography (Dionex, ICS-90, Ion Chromatography system, USA). The mobile phase consisted of a mixture of 7.0 mM sodium carbonate (Na_2CO_3) and 2.0 mM sodium bicarbonate ($NaHCO_3$) delivered at the flow rate of 1.0 mL min^{-1}. AS40 autosampler (Dionex, USA) was assembled with a 10-μL injection loop. A separation column, IonPac® AS9-HC, 4.0 mm × 250 mm (Dionex, USA), a guard column, IonPac® AG9-HC, 4.0 mm × 50 mm (Dionex, USA), and membrane suppressor, AMMS III 4-mm were used. The data acquisition was performed using a Chromeleon 6.5 (Dionex, USA).

2.5. Fluoride sorption studies

The sorption of fluoride on nano-alumina was conducted at room temperature (25 ± 2 °C) by batch experiments. Twenty-five millilitres of fluoride solution of varying initial concentrations (1–100 mg L^{-1}) in 50 mL capped tubes were shaken with 0.025 g of sorbent after adjusting the pH to the desired value, for a specified period of contact time in a temperature controlled shaking assembly. After equilibrium, samples were filtered and the filtrate was then analyzed for residual fluoride concentration by ion chromatography. Reproducibility of the measurements was determined in triplicates and the average values are reported. Relative standard deviations were found to be within ±3.0%. The amount of fluoride sorbed (q_e in mg g^{-1}) was calculated as follows:

$$q_e = \frac{(C_0 - C_e)V}{m} \quad (1)$$

where C_0 and C_e are the initial and final concentrations of fluoride in solution (mg L^{-1}), V is the volume of solution (L) and m is mass of the sorbent (g).

The effect of contact time (1 min to 24 h) was examined with initial fluoride concentrations of 10 and 20 mg L^{-1}. The effect of equilibrium pH was investigated by adjusting solution pH from 3 to 12 using 0.1 M HCl and 0.1 M NaOH under an initial fluoride concentration of 20 mg L^{-1}. The effects of competing anions (chloride, nitrate, carbonate, sulphate and phosphate) on fluoride adsorption were investigated by performing fluoride sorption under a fixed fluoride concentration (20 mg L^{-1}) and initial competing anion concentrations of 20 and 50 mg L^{-1} with sorbent dosage of 1 g L^{-1}.

3. Results and discussion

3.1. Characterization of nano-alumina

The SEM images of pure and fluoride-sorbed nano-alumina are shown in Fig. 1(A) and (B). As can be seen from Fig. 1(A), the sorbent does not possess any well-defined porous structure (only few pores on the surface) and no significant changes were observed in fluoride-sorbed nano-alumina (Fig. 1(B)). The BET surface area of nano-alumina was found to be 151.7 m^2 g^{-1}, whereas the total pore volume was 1.09 cm^3 g^{-1}.

EDX analyses were performed to determine the elemental constituents of pure and fluoride-sorbed nano-alumina (Fig. 2(A) and (B)). It shows that the presence of fluoride in small content appears in the spectrum other than the principal elements Al and O. The wt% of O and Al was found to be 40.79 and 59.21% in pure nano-alumina. Whereas, the EDX results of the fluoride-sorbed

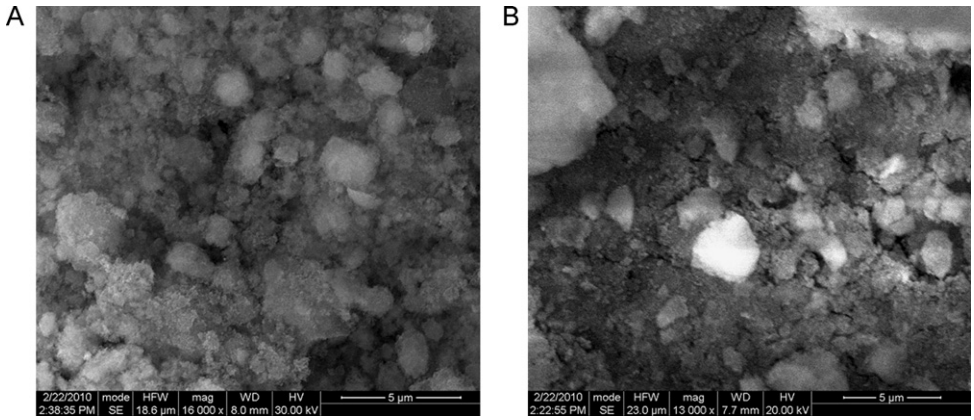

Fig. 1. SEM images of (A) pure nano-alumina; (B) fluoride-sorbed nano-alumina.

nano-alumina showed fluoride peak (1.01% in weight) apart from Al (57.7%) and O (41.29%) peaks. Thus, the EDX results suggest the interaction of fluoride with nano-alumina in the fluoride-sorbed nano-alumina sample.

The XRD patterns of the nano-alumina before and after sorption with fluoride were also recorded. Fig. 3(A) and (B) presents the X-ray diffractograms of original and fluoride-sorbed nano-alumina sample. The peaks of the original sample correspond to those of γ-alumina. The similarity between the diffractograms of the original and the fluoride-sorbed sample indicates that no significant bulk structural changes occurred at that fluorination level (measured fluoride incorporation was 1.01% in weight as obtained by EDX results) and the fluoride ions do not change the phase of γ-alumina.

The FTIR spectra of pure and fluoride-sorbed nano-alumina is shown in Fig. 4(A) and (B). In FTIR spectra of pure nano-alumina (before adsorption) (Fig. 4A), the peak at 3500 cm^{-1} is attributed to the atmospheric water vapor. An absorption band at ca. 1620 cm^{-1} was also observed which is in accordance with the reported literature that alumina presents an absorption band at ca. 1620 cm^{-1} [29]. The peak at 1040 cm^{-1} corresponds to the Al–O stretching vibration [30]. After adsorption of fluoride ions (Fig. 4B), the peaks corresponding to hydroxyl remains unaffected. However, the peak intensity at 1040 cm^{-1} is decreased and a new broad peak appeared in the region of 500–800 cm^{-1}. The decrease in the intensity of 1040 cm^{-1} peak indicated the involvement of the Al–O bonds in the interaction with fluoride ions. The new broad peak in the region of 500–800 cm^{-1} is due to the Al–F stretching vibrations [31] which can be attributed to the complexation of fluoride ions with Al. These observations suggest possible interaction between fluoride and nano-alumina.

3.2. Effect of contact time and initial fluoride concentration

The sorption of fluoride on nano-alumina was investigated as a function of contact time (1 min to 24 h) at two different initial fluoride concentrations (10 and 20 mg L^{-1}). It was noticed that fluoride removal increased with time (Fig. 5). The adsorbent exhibited an initial rapid uptake of fluoride followed by a slower removal rate that gradually reached an equilibrium condition. More than 85% removal of fluoride was attained within first 120 min of contact time and equilibrium was achieved in 24 h. A similar trend of fast kinetics was also observed onto nano-scale aluminum oxide hydroxide during fluoride sorption [25].

The kinetics of fluoride sorption by nano-alumina was also studied at two different initial fluoride concentrations (10 and 20 mg L^{-1}) (Fig. 5). It was observed that fluoride uptake by nano-alumina increased with increase in initial fluoride concentration from 10 to 20 mg L^{-1} (Fig. 5). With the increase in initial fluoride concentration (C_0) from 10 to 20 mg L^{-1}, both fluoride equilibrium concentration (C_e) and equilibrium adsorption capacity (q_e) exhibited increasing trends. These phenomena occurred as the results of the increase in the driving force provided by the concentration gradient with the increase in the initial fluoride concentration (C_0). In contrast, the percentage of fluoride removal showed a decreasing trend. Most fluoride interacted with the binding sites at low initial fluoride concentration, leading to the high percentage of fluoride removal, while only part of fluoride combined with the finite

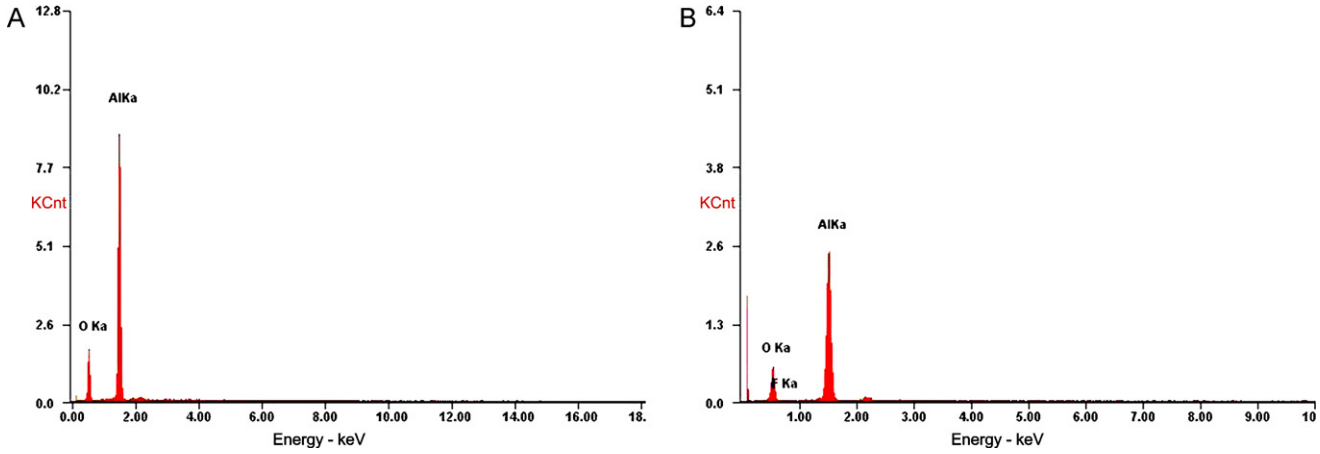

Fig. 2. EDX spectra of (A) pure nano-alumina; (B) fluoride-sorbed nano-alumina (K: the K shell, a: alpha X-ray line (i.e. the type of peak)).

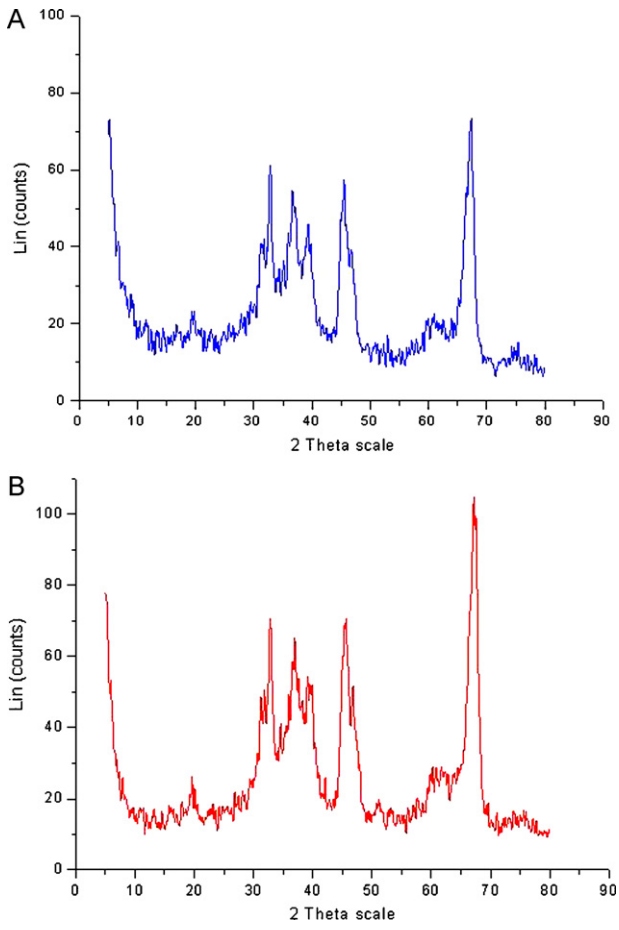

Fig. 3. XRD pattern of (A) pure nano-alumina (reprinted from [27] with permission from Elsevier); (B) fluoride-sorbed nano-alumina.

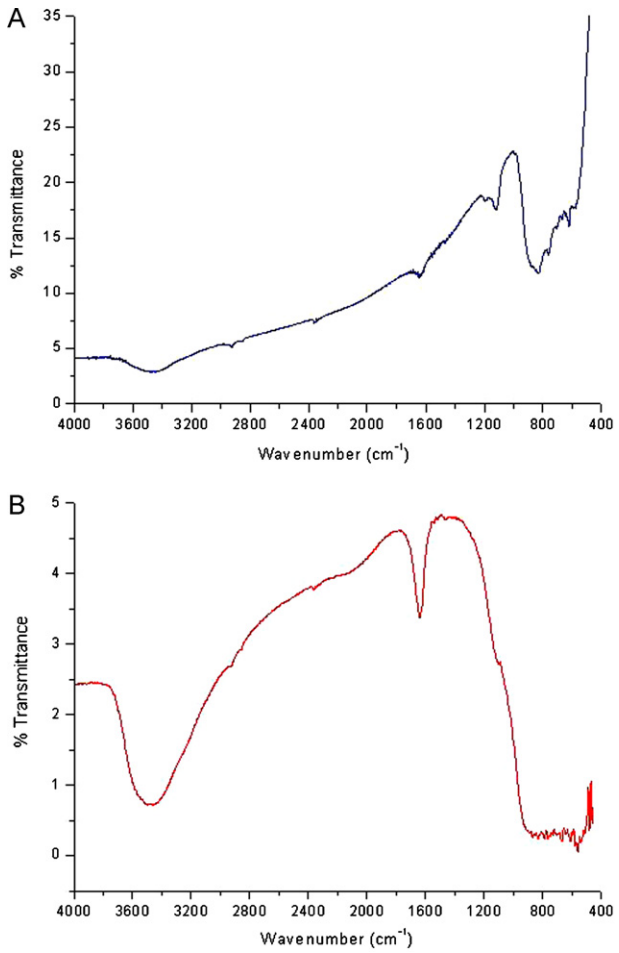

Fig. 4. FTIR spectra of (A) pure nano-alumina (reprinted from [27] with permission from Elsevier); (B) fluoride-sorbed nano-alumina.

binding sites at high initial fluoride concentration, resulting in the relatively low percentage of fluoride removal [32]. These results are similar to those previously reported for the removal of fluoride by different adsorbents [24,32,33].

3.3. Kinetic modeling

The kinetics of fluoride sorption on nano-alumina was analyzed using pseudo-first-order [34] and pseudo-second-order [35] kinetic models to identify the dynamics of the solute adsorption process. The best-fit model, i.e. pseudo-second-order model (Fig. 6) was selected based on the match between experimental ($q_{e(exp)}$) and theoretical ($q_{e(cal)}$) uptake values and linear correlation coefficient (R^2) values at two studied concentrations. The rate equations and the related values are given in Table 1. The values obtained by pseudo-second-order model were found to be in good agreement with experimental data and can be used to favourably explain the fluoride sorption on nano-alumina.

Table 1
Comparison of pseudo-first-order and pseudo-second-order models parameters, and calculated $q_{e(cal)}$ and experimental $q_{e(exp)}$ values for different initial fluoride concentrations.

Pseudo-first-order model: $\log(q_e - q_t) = \log q_e - (k_f/2.303)t$				
C_0 (mg L^{-1})	$q_{e(exp)}$ (mg g^{-1})	k_f (min^{-1})	$q_{e(cal)}$ (mg g^{-1})	R^2
10	5.30	4.37×10^{-2}	2.64	0.8714
20	9.43	2.87×10^{-2}	4.83	0.8672
Pseudo-second-order model: $t/q_t = (1/k_s q_e^2) + (1/q_e)t$				
C_0 (mg L^{-1})	$q_{e(exp)}$ (mg g^{-1})	k_s (g mg^{-1} min^{-1})	$q_{e(cal)}$ (mg g^{-1})	R^2
10	5.30	8.36×10^{-2}	5.33	0.9995
20	9.43	6.06×10^{-2}	9.63	0.9985

q_e: amount of fluoride adsorbed on nano-alumina (mg g^{-1}) at equilibrium; q_t: amount of fluoride adsorbed on nano-alumina (mg g^{-1}) at time t (min); k_f: rate constant for the pseudo-first-order kinetics; k_s: rate constant for the pseudo-second-order kinetics.

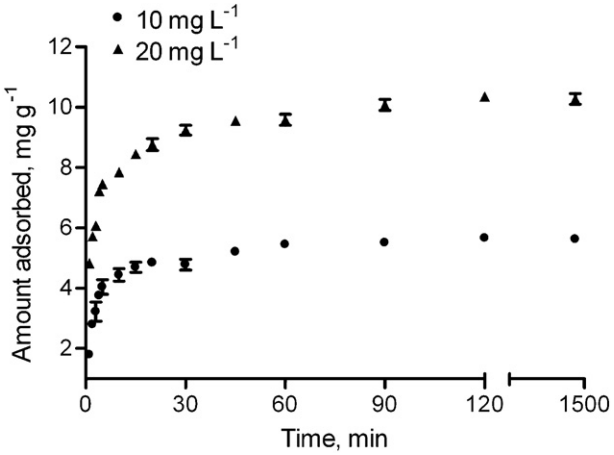

Fig. 5. Effect of contact time and initial fluoride concentration on fluoride sorption on nano-alumina (temperature = 25 °C; sorbent dose = 1 g L^{-1}; pH = 6.15 ± 0.21; agitation speed = 220 rpm).

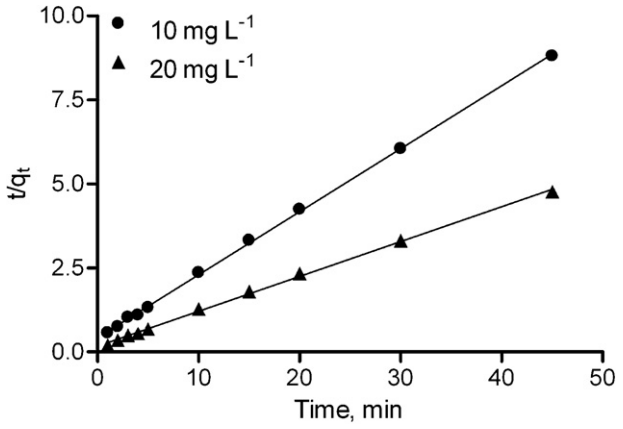

Fig. 6. Pseudo-second-order kinetic plots of fluoride sorption on nano-alumina.

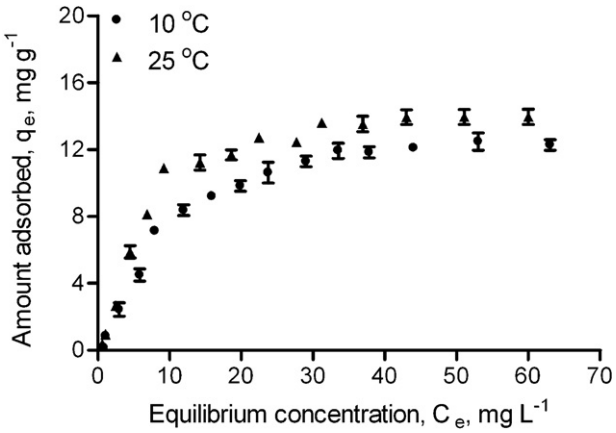

Fig. 8. Sorption isotherms of fluoride sorption on nano-alumina (contact time = 24 h; sorbent dose = 1 g L^{-1}; pH = 6.15; agitation speed = 220 rpm).

3.4. Effect of pH

The pH is an important parameter influencing the sorption process at the water–sorbent interfaces. To determine the optimum pH for the maximum removal of fluoride, the equilibrium sorption of fluoride (with initial fluoride concentration of 20 mg L^{-1}) was investigated over a pH range of 3–12. It can be seen (Fig. 7) that the sorption of fluoride on nano-alumina is strongly pH dependent. The sorption of fluoride increases with increased pH, reaching a maximum at pH 6.15, and then decreased with further increase in pH. Initially, as the pH increased from 3 to 6.15, the fluoride sorption also increased due to the fact that for pH < pH_{pzc} (7.2), the surface of nano-alumina becomes positively charged and attracts negative fluoride anions, and becomes maximum at pH 6.15. The decrease in sorption capacity at pH greater than 6.15 can be attributed to the competition for the active sites by OH^- ions and the electrostatic repulsion of anionic fluoride by the negatively charged Al_2O_3 surface. The minimal fluoride removal capacity in acidic pH is presumably due to the formation of HF, which reduces the coulombic attraction between fluoride and the adsorbent surface [2].

3.5. Sorption isotherms

In order to evaluate the sorption capacity of nano-alumina for fluoride, the equilibrium sorption of fluoride was studied as a function of fluoride concentration and the sorption isotherms are shown in Fig. 8. A sorption capacity of ca. 14.0 mg g^{-1} was observed for fluoride on nano-alumina at 25 °C. It can be found (Fig. 8) that the sorption capacity at equilibrium gradually increased with the increase in equilibrium fluoride concentrations. The gradual rise in the isotherm indicates the availability of readily accessible sites for sorption during the initial phase. However, site saturation occurs as the fluoride concentration increases and a plateau is reached indicating that no more sites remain available for sorption.

The mechanism of fluoride removal process has been shown to involve the replacement of OH^- with F^- [36]. Fluoride ions and hydroxide ions form $Al_nF_m(OH)_{3n-m}$ complexes with Al(III) ions as given in Eq. (2) [36].

$$nAl^{3+}_{(aq)} + 3n - mOH^-_{(aq)} + mF^-_{(aq)} \rightarrow Al_nF_m(OH)_{3n-m(s)} \quad (2)$$

Zhang et al. [37] studied the interaction of fluoride on γ-alumina surface by multinuclear MAS NMR spectroscopy to identify the fluorine species on the fluorinated γ-alumina. The spectroscopic analysis indicated that fluorine enters the surface of alumina by substituting hydroxyl groups without breaking the bridging Al–O–Al bonds. At higher fluoride loadings, bridging Al–O–Al bonds were found to be broken to sorb more fluoride under the strong electron-withdrawing effect of fluorine. It is expected that similar processes occur on nano-alumina.

Adsorption potential of nano-alumina in the present study was compared with other adsorbents reported in previous studies for fluoride removal and is compiled in Table 2. It is seen that nano-alumina used in the present study shows comparable adsorption capacity for fluoride removal compared to some previously developed adsorbents. However, in some cases, it shows lower sorption potential towards fluoride and research is being focused now to enhance the adsorption potential of nano-alumina by chemical modifications.

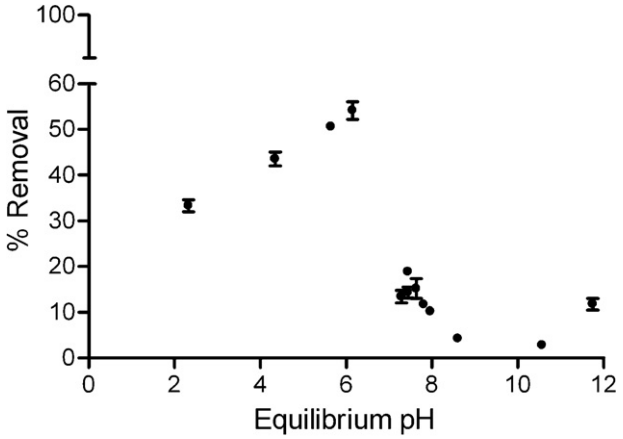

Fig. 7. Effect of pH on fluoride sorption on nano-alumina (C_0 = 20 mg L^{-1}; temperature = 25 °C; contact time = 24 h; sorbent dose = 1 g L^{-1}; agitation speed = 220 rpm).

3.6. Effect of temperature on fluoride sorption by nano-alumina

In order to investigate the effect of temperature on fluoride removal by nano-alumina, sorption experiments were also performed at 10 °C. A comparison of sorption isotherms at 10 and 25 °C indicates that fluoride sorption by nano-alumina is not significantly affected by temperature variation (Fig. 8).

The sorption data was further analyzed using two well known isotherm models, viz. Langmuir and Freundlich models, which can be expressed by Eqs. (3) and (4):

$$\frac{1}{q_e} = \frac{1}{q_m} + \frac{1}{q_m b C_e} \quad (3)$$

$$\log q_e = \log K_F + \frac{1}{n} + \log C_e \quad (4)$$

Table 2
Comparison of efficiency of various adsorbents for fluoride removal from water.

Adsorbent	Amount adsorbed ($mg\,g^{-1}$)	Experimental conditions	Reference
$KMnO_4$ modified carbon	15.9	pH: 2.0 Concentration: 5–20 $mg\,L^{-1}$ Temperature: 25 °C	[7]
Granular ferric hydroxide (GFH)	7.0	pH: 6.0–7.0 Concentration: 1–100 $mg\,L^{-1}$ Temperature: 25 °C	[16]
Fe_3O_4@$Al(OH)_3$ magnetic nanoparticles	88.48	pH: 6.5 Concentration: 0–160 $mg\,L^{-1}$ Temperature: 25 °C	[24]
Granular activated alumina (PURALOX) Copper oxide coated alumina	2.232 7.220	Concentration: 10 $mg\,L^{-1}$ Temperature: 30 ± 1 °C	[43]
Iron(III)–Tin(IV) mixed oxide	10.47	pH: 6.4 Concentration: 10–50 $mg\,L^{-1}$ Temperature: 303 K	[44]
Fe–Al–Ce nano-adsorbent	2.22	pH: 7.0 Concentration: 0.0001 M Temperature: 25 °C	[45]
Scandinavia spruce wood charcoal (AlFe650/C)	13.64	pH: 7.0 Temperature: 28 ± 2 °C Concentration: 2–50 $mg\,L^{-1}$	[46]
Acid treated spent bleaching earth	7.752	pH: 3.5 Concentration: 5–45 $mg\,dm^{-3}$	[47]
Chemical treated laterite	37.9	pH: 5.0 Concentration: 3–50 $mg\,L^{-1}$ Temperature: 305 K	[48]
Magnetic-chitosan	22.49	pH: 7.0 Concentration: 5–140 $mg\,L^{-1}$	[49]
Hydrous-manganese-oxide-coated alumina	7.09	pH: 5.2 Concentration: 10–70 $mg\,L^{-1}$ Temperature: 30 °C	[50]
Hydrotalcite/chitosan composite	1.255	Temperature: 30 °C Concentration: upto 15 $mg\,L^{-1}$ pH: acidic pH	[51]
Granular ceramic	12.12	Temperature: 20 °C Concentration: 5–50 $mg\,L^{-1}$ pH: 6.90	[52]
Nano-alumina	14.0	pH: 6.15 Concentration: 1–100 $mg\,L^{-1}$ Temperature: 25 °C	Present work

where q_e is amount sorbed at equilibrium concentration C_e, q_m is the Langmuir constant representing maximum monolayer sorption capacity, b is the Langmuir constant related to energy of sorption, K_F and $1/n$ are Freundlich constants, associated with adsorption capacity and adsorption intensity, respectively.

The experimental data did not fit well with the Freundlich model (see Table 3) but was fitted well with Langmuir model. The plots of $1/q_e$ as a function of $1/C_e$ for the sorption of fluoride on nano-alumina are shown in Fig. 9. The values of q_m and b are given in Table 3. The values of q_m calculated by the Langmuir isotherm were all close to experimental values at given temperatures. These facts suggest that fluoride is sorbed in the form of monolayer coverage on the surface of the sorbent.

The influence of sorption isotherm shape has been discussed [38] to examine whether sorption is favorable in terms of 'R_L', a dimensionless constant referred to as separation factor or equilibrium parameter. 'R_L' is calculated using the following equation:

$$R_L = \frac{1}{1 + bC_0} \quad (5)$$

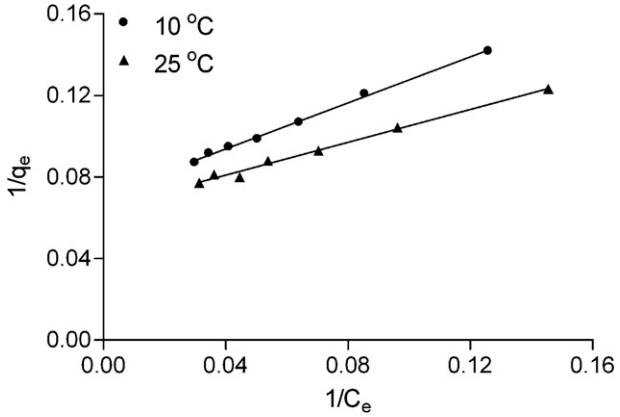

Fig. 9. Langmuir isotherm of fluoride sorption on nano-alumina.

Table 3
Langmuir and Freundlich constants for the adsorption of fluoride on nano-alumina at 10 and 25 °C.

Temperature (°C)	Langmuir constants				Freundlich constants		
	q_m ($mg\,g^{-1}$)	b ($L\,mol^{-1}$)	R_L	R^2	$1/n$	K_F ($mg\,g^{-1}$)($L\,mg^{-1}$)$^{1/n}$	R^2
10	14.10	2.36×10^3	0.31	0.9980	0.94	0.81	0.9823
25	15.43	3.24×10^3	0.27	0.9912	0.98	1.01	0.9626

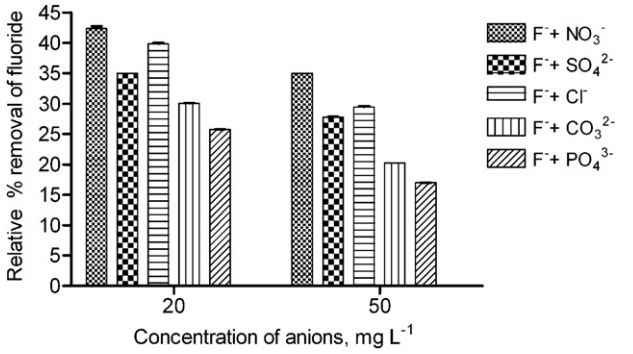

Fig. 10. Effect of different concentrations of competitive anions on fluoride sorption on nano-alumina (temperature = 25 °C; contact time = 24 h; sorbent dose = 1 g L^{-1}; agitation speed = 220 rpm).

The R_L values obtained are compiled in Table 3. Both the R_L values lie between 0 and 1 confirming that the adsorption isotherm is favorable.

3.7. Thermodynamic parameters

The nature and thermodynamic feasibility of the sorption process were determined by evaluating the thermodynamic constants, standard free energy (ΔG°), standard enthalpy (ΔH°) and standard entropy (ΔS°) using the following equations:

$$\Delta G^\circ = -RT\ln(K) \quad (6)$$

$$\ln\frac{K_2}{K_1} = \frac{\Delta H^\circ}{R}\left(\frac{1}{T_1} - \frac{1}{T_2}\right) \quad (7)$$

$$\Delta G^\circ = \Delta H^\circ - T\Delta S^\circ \quad (8)$$

where R is the universal gas constant (8.314 J mol^{-1} K^{-1}), T is the temperature in Kelvin and K is the equilibrium constant, related to the Langmuir constant 'b' via Eq. (9), where the value 55.5 corresponds to the molar concentration of the solvent (in this case water) with units of mol L^{-1} [39,40].

$$K = b \times 55.5 \quad (9)$$

The sorption process is spontaneous in nature, as indicated by the negative value of ΔG° (−29.97 kJ mol^{-1}) at 298 K. The positive value of ΔH° for fluoride adsorption is 14.81 kJ mol^{-1}, suggesting that the interaction of fluoride and nano-alumina is endothermic in nature. Affinity of the sorbent for fluoride is represented by the positive value of ΔS° (150.3 J mol^{-1} K^{-1}).

3.8. Effect of competing anions on fluoride adsorption by nano-alumina

The influence of various anions present in groundwater such as, chloride (Cl^-), nitrate (NO_3^-), sulphate (SO_4^{2-}), carbonate (CO_3^{2-}) and phosphate (PO_4^{3-}) on fluoride removal by nano-alumina was investigated at 20 mg L^{-1} of initial fluoride concentration (Fig. 10). The concentrations of competing anions were 20 and 50 mg L^{-1}. It was found that anions present in fluoride solution are likely to limit the fluoride removal efficiency. Fluoride sorption was mainly influenced by the presence of phosphate followed by carbonate and sulphate. In the presence of phosphate, relative percent removal of fluoride was ~26% and 17% at 20 and 50 mg L^{-1}, respectively, while in case of sulphate and carbonate, relative percent removal of fluoride was ~35% and 30% and 27% and 20% at 20 and 50 mg L^{-1}, respectively. The fluoride removal was decreased in presence of phosphate and sulphate which indicates that the inner-spherically sorbing anions, phosphate and sulphate [41,42] can significantly interfere the sorption of fluoride where the sorption competition occurred for the limited amount of sorption sites on nano-alumina. The decrease in fluoride adsorption in presence of carbonate was presumably due to the significant increase in pH of the solution. It was also confirmed from our experiments on the effect of pH (Section 3.4) that the fluoride removal decreases in highly alkaline pH. Furthermore, fluoride sorption was least influenced in presence of chloride and nitrate (outer-spherically sorbing anions).

4. Conclusions

The results from the present study exhibit the potential of nano-alumina for fluoride removal from aqueous solutions. The sorption of fluoride on nano-alumina was found to be strongly pH dependent with maximum fluoride removal occurring at pH 6.15. Kinetic analyses indicate that the sorption process followed pseudo-second-order kinetics under the selected concentration range. The sorption capacity of nano-alumina for fluoride was found to be ca. 14.0 mg g^{-1} at 25 °C. The sorption isotherm was fitted well with Langmuir model. The FTIR and EDX results provide an evidence of the interaction between fluoride and nano-alumina moieties resulting in the formation of aluminum-fluoro complexes. Fluoride sorption was influenced more by the presence of PO_4^{3-}, SO_4^{2-} and CO_3^{2-}.

Acknowledgments

A part of this research work was partially conducted at Institute of Environmental Technology and Energy Economics (IUE), TUHH, Hamburg-Harburg, Germany and authors express their sincere thanks to IUE staff for providing necessary help. One of the authors (AB) is also thankful to FCT (Fundação para a Ciência e a Technologia), Lisbon, Portugal, for the award of post-doctoral grant (FCT-DFRH-SFRH/BPD/62889/2009).

References

[1] D.P. Das, J. Das, K. Parida, Physicochemical characterization and adsorption behavior of calcined Zn/Al hydrotalcite-like compound (HTlc) towards removal of fluoride from aqueous solution, J. Colloid Interface Sci. 261 (2003) 213–220.
[2] A.M. Raichur, M.J. Basu, Adsorption of fluoride onto mixed rare earth oxides, Sep. Purif. Technol. 24 (2001) 121–127.
[3] F. Shen, X. Chen, P. Gao, G. Chen, Electrochemical removal of fluoride ions from industrial wastewater, Chem. Eng. Sci. 58 (2003) 987–993.
[4] WHO (World Health Organization), Guidelines for Drinking-Water Quality [Electronic Resource]: Incorporating First Addendum (vol. I) Recommendations, 2006, pp. 375–377.
[5] P.T.C. Harrison, Fluoride in water: a UK perspective, J. Fluorine Chem. 126 (2005) 1448–1456.
[6] S. Ghorai, K.K. Pant, Investigations on the column performance of fluoride adsorption by activated alumina in a fixed-bed, Chem. Eng. J. 98 (2004) 165–173.
[7] A.A.M. Daifullah, S.M. Yakout, S.A. Elreefy, Adsorption of fluoride in aqueous solutions using $KMnO_4$-modified activated carbon derived from steam pyrolysis of rice straw, J. Hazard. Mater. 147 (2007) 633–643.
[8] S. Saha, Treatment of aqueous effluent for fluoride removal, Water Res. 27 (1993) 1347–1350.
[9] K. Vaaramaa, J. Lehto, Removal of metals and anions from drinking water by ion exchange, Desalination 155 (2003) 157–170.
[10] Z. Amor, B. Bariou, N. Mameri, M. Taky, S. Nicolas, A. Elmidaoui, Fluoride removal from brackish water by electrodialysis, Desalination 133 (2001) 215–223.
[11] P.I. Ndiaye, P. Moulin, L. Dominguez, J.C. Millet, F. Charbit, Removal of fluoride from electronic industrial effluent by RO membrane separation, Desalination 173 (2005) 25–32.
[12] G. Moges, F. Zewge, M. Socher, Preliminary investigations on the defluoridation of water using fired clay chips, J. Afr. Earth Sci. 21 (1996) 479–482.
[13] Y. Wang, E.J. Reardon, Activation and regeneration of a soil sorbent for defluoridation of drinking water, Appl. Geochem. 16 (2001) 531–539.
[14] D.S. Bhargava, D.J. Killedar, Fluoride adsorption on fishbone charcoal through a moving media adsorber, Water Res. 26 (1992) 781–788.
[15] M.S. Onyango, Y. Kojima, A. Kumar, D. Kuchar, M. Kubota, H. Matsuda, Uptake of fluoride by Al^{3+}-pretreated low-silica synthetic zeolites: adsorption equilibrium and rate studies, Sep. Sci. Technol. 41 (2006) 683–704.

[16] E. Kumar, A. Bhatnagar, M. Ji, W. Jung, S. Lee, S.J. Kim, G. Lee, H. Song, J.Y. Choi, J. Yang, B.H. Jeon, Defluoridation from aqueous solutions by granular ferric hydroxide (GFH), Water Res. 43 (2009) 490–498.
[17] S.V. Mohan, S.V. Ramanaiah, B. Rajkumar, P.N. Sarma, Removal of fluoride from aqueous phase by biosorption onto algal biosorbent *Spirogyra* sp.-*IO2*: sorption mechanism elucidation, J. Hazard. Mater. 141 (2007) 465–474.
[18] M. Zhu, M. Xie, X. Jiang, Interaction of fluoride with hydroxyaluminum–montmorillonite complexes and implications for fluoride-contaminated acidic soils, Appl. Geochem. 21 (2006) 675–683.
[19] USEPA, Water treatment technology feasibility support document for chemical contaminants, in: Support of EPA Six-year Review of National Primary Drinking Water Regulations, EPA 815-R-03-004, 2003.
[20] P. Jovančić, M. Radetić, in: D. Barceló, M. Petrovic (Eds.), Emerging Contaminants from Industrial and Municipal Waste: Removal Technologies (The Handbook of Environmental Chemistry/Water Pollution), vol. 5, Springer-Verlag, Berlin, Heidelberg, 2008, pp. 239–264.
[21] K. Hristovski, A. Baumgardner, P. Westerhoff, Selecting metal oxide nanomaterials for arsenic removal in fixed bed columns: from nanopowders to aggregated nanoparticle media, J. Hazard. Mater. 147 (2007) 265–274.
[22] P. Puttamraju, A.K. SenGupta, Evidence of tunable on-off sorption behaviors of metal oxide nanoparticles: role of ion exchanger support, Ind. Eng. Chem. Res. 45 (2006) 7737–7742.
[23] X. Zhao, Y. Shi, Y. Cai, S. Mou, Cetyltrimethylammonium bromide-coated magnetic nanoparticles for the preconcentration of phenolic compounds from environmental water samples, Environ. Sci. Technol. 42 (2008) 1201–1206.
[24] X. Zhao, J. Wang, F. Wu, T. Wang, Y. Cai, Y. Shi, G. Jiang, Removal of fluoride from aqueous media by Fe_3O_4@$Al(OH)_3$ magnetic nanoparticles, J. Hazard. Mater. 173 (2010) 102–109.
[25] S.-G. Wang, Y. Ma, Y.-J. Shi, W.-X. Gong, Defluoridation performance and mechanism of nano-scale aluminum oxide hydroxide in aqueous solution, J. Chem. Technol. Biotechnol. 84 (2009) 1043–1050.
[26] G. Patel, U. Pal, S. Menon, Removal of fluoride from aqueous solution by CaO nanoparticles, Sep. Sci. Technol. 44 (2009) 2806–2826.
[27] A. Bhatnagar, E. Kumar, M. Sillanpää, Nitrate removal from water by nano-alumina: characterization and sorption studies, Chem. Eng. J. 163 (2010) 317–323.
[28] D.H. Lataye, I.M. Mishra, I.D. Mall, Removal of pyridine from aqueous solution by adsorption on bagasse fly ash, Ind. Eng. Chem. Res. 45 (2006) 3934–3943.
[29] T. Tsuchida, Preparation and reactivity of acicular α-Al_2O_3 from synthetic diaspore, β-$Al_2O_3 \cdot H_2O$, Solid State Ionics 63 (1993) 464–470.
[30] M. Zhareslu, M. Crisan, M. Preda, V. Fruth, S. Preda, Al_2TiO_5-based ceramics obtained by hydrothermal process, J. Optoelctron. Adv. Mater. 5 (2003) 1411–1416.
[31] W. Kleist, C. Haebner, O. Storcheva, C. Kohler, A simple aqueous phase synthesis of high surface area aluminum fluoride and its bulk and surface structure, Inorg. Chim. Acta 359 (2006) 4851–4854.
[32] Q. Liu, H. Guo, Y. Shan, Adsorption of fluoride on synthetic siderite from aqueous solution, J. Fluorine Chem. 131 (2010) 635–641.
[33] N. Viswanathan, C.S. Sundaram, S. Meenakshi, Removal of fluoride from aqueous solution using protonated chitosan beads, J. Hazard. Mater. 161 (2009) 423–430.
[34] S. Lagergren, About the theory of so-called adsorption of soluble substances, K. Svenska Vetenskapsakad Handl. 24 (1898) 1–39.
[35] Y.S. Ho, G. McKay, Pseudo-second-order model for sorption processes, Process Biochem. 34 (1999) 451–465.
[36] C.Y. Hu, S.L. Lo, W.H. Kuan, Effects of the molar ratio of hydroxide and fluoride to Al(III) on fluoride removal by coagulation and electrocoagulation, J. Colloid Interface Sci. 283 (2005) 472–476.
[37] W. Zhang, M. Sun, R. Prins, Multinuclear MAS NMR identification of fluorine species on the surface of fluorinated γ-alumina, J. Phys. Chem. B 106 (2002) 11805–11809.
[38] T.W. Weber, R.K. Chakravorti, Pore and solid diffusion models for fixed bed adsorbents, J. Am. Inst. Chem. Eng. 20 (1974) 228–238.
[39] R.J. Hunter, Foundations of Colloid Science, Oxford University Press, Oxford, 2001.
[40] A.M. Vasilev, J. Ralston, D.A. Beattie, Adsorption of modified dextrins on talc: effect of surface coverage and hydration water on hydrophobicity reduction, Langmuir 24 (2008) 6121–6127.
[41] S. Goldberg, G. Sposito, A chemical model of phosphate adsorption by soils. I. Reference oxides minerals, Soil Sci. Soc. Am. J. 48 (1984) 772–778.
[42] P.C. Zhang, D.L. Spark, Kinetics and mechanisms of sulfate adsorption/desorption on goethite using pressure-jump relaxation, Soil Sci. Soc. Am. J. 54 (1990) 1266–1273.
[43] A. Bansiwal, P. Pillewan, R.B. Biniwale, S.S. Rayalu, Copper oxide incorporated mesoporous alumina for defluoridation of drinking water, Micropor. Mesopor. Mater. 129 (2010) 54–61.
[44] K. Biswas, K. Gupta, U.C. Ghosh, Adsorption of fluoride by hydrous iron(III)–tin(IV) bimetal mixed oxide from the aqueous solutions, Chem. Eng. J. 149 (2009) 196–206.
[45] L. Chen, H.-X. Wu, T.-J. Wang, Y. Jin, Y. Zhang, X.-M. Dou, Granulation of Fe–Al–Ce nano-adsorbent for fluoride removal from drinking water by spray coating on sand in a fluidized bed, Powder Technol. 193 (2009) 59–64.
[46] E. Tchomgui-Kamga, V. Alonzo, C.P. Nanseu-Njiki, N. Audebrand, E. Ngameni, A. Darchen, Preparation and characterization of charcoals that contain dispersed aluminum oxide as adsorbents for removal of fluoride from drinking water, Carbon 48 (2010) 333–343.
[47] M. Mahramanlioglu, I. Kizilcikli, I.O. Bicer, Adsorption of fluoride from aqueous solution by acid treated spent bleaching earth, J. Fluorine Chem. 115 (2002) 41–47.
[48] A. Maiti, J.K. Basu, S. De, Chemical treated laterite as promising fluoride adsorbent for aqueous system and kinetic modeling, Desalination 265 (2011) 28–36.
[49] W. Ma, F.-Q. Ya, M. Han, R. Wang, Characteristics of equilibrium, kinetics studies for adsorption of fluoride on magnetic-chitosan particle, J. Hazard. Mater. 143 (2007) 296–302.
[50] S.-X. Teng, S.-G. Wang, W.-X. Gong, X.-W. Liu, B.-Y. Gao, Removal of fluoride by hydrous manganese oxide-coated alumina: performance and mechanism, J. Hazard. Mater. 168 (2009) 1004–1011.
[51] N. Viswanathana, S. Meenakshi, Selective fluoride adsorption by a hydrotalcite/chitosan composite, Appl. Clay Sci. 48 (2010) 607–611.
[52] N. Chen, Z. Zhang, C. Feng, N. Sugiura, M. Li, R. Chen, Fluoride removal from water by granular ceramic adsorption, J. Colloid Interface Sci. 348 (2010) 579–584.